Journal of Sound and Vibration (2001) **239**(1), 123–137
doi:10.1006/jsvi.2000.3111, available online at http://www.idealibrary.com on IDEAL®

DYNAMICS OF RECTANGULAR PLATES UNDERGOING PRESCRIBED OVERALL MOTION

H. H. Yoo

School of Mechanical Engineering, Hanyang University, Sungdong-Gu Haengdang-Dong 17, *Seoul*, 133–791, *Republic of Korea. E-mail: hhyoo@email.hanyang.ac.kr*

AND

J. Chung

Department of Mechanical Engineering, Hanyang University, 1271 *Sa*-1-*Dong*, *Ansan*, *Kyunggi-do*, 425–791, *Republic of Korea South*

(*Received* 18 *January* 2000, *and in final form* 31 *May* 2000)

A set of linear equations of motion for rectangular plates undergoing prescribed overall motion is derived in this paper. Two in-plane stretch variables, with which the in-plane strain energy of the plate can be expressed in an exact quadratic form, are employed and approximated to derive the equations of motion. The equations of motion include motion-induced stiffness variation terms, which are expressed as explicit functions of the prescribed overall motion. The effects of the motion-induced stiffness variation terms, which are neglected in the conventional linear modelling method, on the dynamic response of the plate are investigated. The reliability and the accuracy of the equations of motion which are derived in the present work are examined through the numerical study.

1. INTRODUCTION

Flexible structures undergoing overall motion are often found in engineering examples such as turbine blades, aircraft rotary wings, and spacecraft appendages. It is well known that the overall motion (translational or rotational motion) may cause significant variations of dynamic characteristics of the structures. If the variations are not properly considered, erroneous numerical results are often obtained. Therefore, the variations should be accurately estimated and considered for the flexible structures undergoing overall motion.

Flexible structures having slender shapes are often idealized as beams since reliable and robust theories for beams, which can provide accurate numerical results in most cases, are available. Many structures, however, have plate-like shapes (rather than beam-like shapes). Solar panels of satellites, low-pressure stage turbine blades, and aircraft rotary wings with small aspect ratios are such examples. For these structures, numerical results obtained by using beam theories may cause significant errors in estimating their dynamic responses. Therefore, accurate modelling methods for the dynamic analysis of plate-like structures are required.

The modelling method which is most widely used for the dynamic analysis of a flexible structure is often called as the conventional linear modelling method [1–3], which employs Cartesian deformation variables along with the linear Cauchy strain measure. This

0022-460X/01/010123 + 15 $35.00/0

modelling method has several merits such as simplicity of formulation, ease of implementation in finite element methods, and availability of the co-ordinate reduction technique [4], which enables one to save enormous computation time for the dynamic analysis of structures. However, this modelling method often provides erroneous dynamic analysis results for the structures undergoing overall motion. It was found that the modelling method failed to capture proper motion-induced stiffness variation effects (see, for instance, reference [5]). To resolve the problem, several non-linear modelling methods [5–8] were introduced and the accuracy problem (that the conventional linear modelling method entailed) could be remedied. However, enormous computational burden results from the non-linearity of the modelling methods, which disables the co-ordinate reduction technique.

More recently, a new linear modelling method [9, 10] was introduced for the transient analysis of flexible beams undergoing overall motion. Different from the conventional linear modelling method, this linear modelling method employs a non-Cartesian deformation variable which is approximated to derive the equations of motion. It was proved that the use of the non-Cartesian variable led to capture accurate motion-induced stiffness variation effects. Thus, this modelling method is as efficient (due to its linearity) as the conventional linear modelling method and as accurate as the non-linear modelling methods. This modelling method, however, has not been extented to plates so far. Actually, numerical results for the transient analysis of plates undergoing overall motion are rarely available in the literature. Even though a non-linear formulation for plates undergoing overall motion was suggested in reference [11], numerical results were not given in the work. Some numerical results for the vibration analysis of rotating plates are available in references [12, 13].

The purpose of this paper is to present an accurate and efficient linear-modelling method for plates undergoing prescribed overall motion. The key ingredient of the modelling method is the use of two stretch variables which are to be approximated. The use of the two stretch variables enables one to derive linear equations of motion which include proper motion-induced stiffness variation terms due to overall motion. This modelling method is the extension of the modelling method for beams introduced in reference [10]. The accuracy of the present modelling method is examined by comparing its results with some existing results. Numerical results obtained by using the present modelling method are also compared with those obtained by using the conventional linear modelling method so that the importance of the motion-induced stiffness variation effects can be clearly exhibited.

2. EQUATIONS OF MOTION

In this section, equations of motion of a rectangular plate undergoing prescribed overall motion are derived. The following assumptions are made. The plate has homogeneous and isotropic material properties. The thickness of the plate is uniform and small compared to other dimensions of the plate so that the Kirchhoff hypothesis can be employed. So the transverse shear and the rotary inertia effects are neglected in this work. These assumptions are made to simplify the formulation and focus on the major issue of the present work, which is involved with the stiffness variation due to overall motion.

Figure 1 shows a rectangular plate which has uniform thickness. By the Kirchhoff hypothesis, any straight line segments perpendicular to the midplane of the plate before deformation remain perpendicular to the midplane after deformation. Therefore, any one of them can be used as a rigid reference frame for the plate. In this work, the straight line segment at a corner of the rectangular plate is used as the reference frame of the plate as shown in the figure. A unit vector triad ($\hat{a}_1$, $\hat{a}_2$, and $\hat{a}_3$) is fixed to the reference frame.

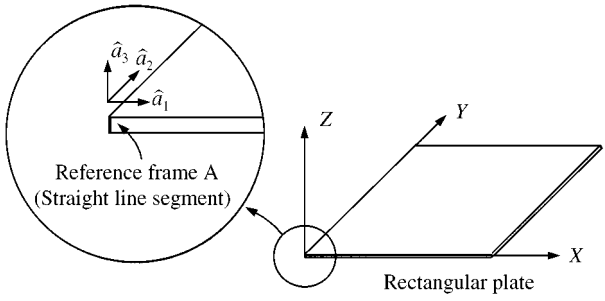

Figure 1. Rectangular plate and its reference frame.

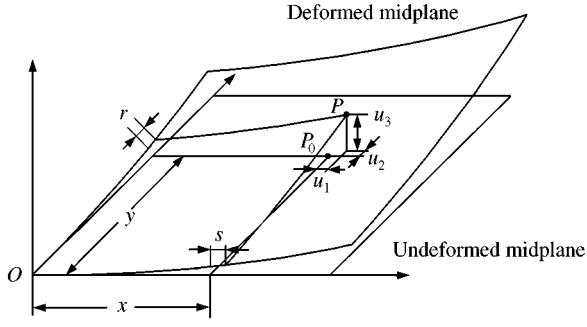

Figure 2. Deformation variables for a rectangular plate.

Figure 2 shows the midplanes of a rectangular plate before and after deformation. The elastic deformation of a generic point in the midplane is denoted as **u** (vector from point P_0 to point P shown in the figure). Three Cartesian variables (u_1, u_2, and u_3 as shown in the figure) are employed to express the elastic deformation vector. Conventionally, the three Cartesian deformation variables are approximated to obtain ordinary differential equations of motion. In the present study, however, u_1 and u_2 are not approximated while u_3 is approximated. Instead, two in-plane stretch variables (s and r shown in the figure) are approximated. Thus, by using the Rayleigh–Ritz method, they can be expressed as follows:

$$s(x, y, t) = \sum_{j=1}^{\mu} \phi_{1j}(x, y) q_j(t), \tag{1}$$

$$r(x, y, t) = \sum_{j=1}^{\mu} \phi_{2j}(x, y) q_j(t), \tag{2}$$

$$u_3(x, y, t) = \sum_{j=1}^{\mu} \phi_{3j}(x, y) q_j(t), \tag{3}$$

where ϕ_{1j}, ϕ_{2j}, and ϕ_{3j} are spatial mode functions. Any compact set of admissible functions which satisfy the geometric boundary conditions of the plate can be used as the mode functions (see reference [14]). In the present work, the eigenfunctions of rectangular plates (with no overall motion) are employed as the mode functions. q_j's are generalized co-ordinates and μ is the total number of the generalized co-ordinates. For the convenience of formalism, s, r, and u_3 use the same number of co-ordinates μ. However, they are not actually coupled. For instance, ϕ_{1j} is not zero only if $j \leqslant \mu_1$; ϕ_{2j} is not zero only if

$\mu_1 < j \leqslant \mu_1 + \mu_2$; and ϕ_{3j} is not zero only if $\mu_1 + \mu_2 < j \leqslant \mu_1 + \mu_2 + \mu_3$. In other words, μ_1, μ_2, and μ_3 denote the actual number of generalized co-ordinates for s, r, and u_3 respectively. μ is the total sum of μ_1, μ_2, and μ_3.

The strain energy of a plate can be expressed as follows:

$$U = U_i + U_b, \tag{4}$$

where U_i and U_b represent the in-plane and the bending strain energies which are expressed (by employing the deformation variables s, r, and u_3) as follows:

$$U_i = \tfrac{1}{2}\int_0^b \int_0^a \left[\beta_1 \left\{ \left(\frac{\partial s}{\partial x}\right)^2 + \left(\frac{\partial r}{\partial y}\right)^2 + 2v\left(\frac{\partial s}{\partial x}\right)\left(\frac{\partial r}{\partial y}\right) \right\} + \beta_2 \left(\frac{\partial s}{\partial y} + \frac{\partial r}{\partial x}\right)^2 \right] \mathrm{d}x\,\mathrm{d}y, \tag{5}$$

$$U_b = \tfrac{1}{2}\int_0^b \int_0^a \beta_3 \left[\left(\frac{\partial^2 u_3}{\partial x^2}\right)^2 + \left(\frac{\partial^2 u_3}{\partial y^2}\right)^2 + 2v\left(\frac{\partial^2 u_3}{\partial x^2}\right)\left(\frac{\partial^2 u_3}{\partial y^2}\right) + 2(1-v)\left(\frac{\partial^2 u_3}{\partial x \partial y}\right)^2 \right] \mathrm{d}x\,\mathrm{d}y, \tag{6}$$

where a and b denote the length and the width of the plate, and

$$\beta_1 = \frac{Eh}{(1-v^2)}, \tag{7}$$

$$\beta_2 = Gh, \tag{8}$$

$$\beta_3 = \frac{Eh^3}{12(1-v^2)}, \tag{9}$$

where E, G, v, and h represent Young's modulus, the shear modulus, Poisson ratio, and the thickness of the plate respectively. Since the stretch variables s and r are employed, equation (5) represents the exact in-plane strain energy of the plate.

By using the strain energies given in equations (5) and (6), the generalized active forces (see reference [15]) can be obtained as follows:

$$F_i = -\frac{\partial U}{\partial q_i}, \quad (i = 1, 2, \ldots, \mu). \tag{10}$$

The use of s and r results in the exact in-plane strain energy which is expressed in a quadratic form. Thus, linear generalized active forces can be obtained. It, however, complicates the formulation of generalized inertia forces in the equations of motion. The generalized inertia forces (see reference [15]) can be obtained by using the following equation:

$$F_i^* = -\int_0^b \int_0^a \rho \left(\frac{\partial \mathbf{v}^P}{\partial \dot{q}_i}\right) \cdot \mathbf{a}^P \,\mathrm{d}x\,\mathrm{d}y \quad (i = 1, 2, \ldots, \mu), \tag{11}$$

where ρ is the mass per unit area of the plate; $\dot{q}_i$'s are the time derivatives of the generalized coordinates; and $\mathbf{v}^P$ and $\mathbf{a}^P$ are the velocity and the acceleration of the generic point P. The velocity of point P can be obtained from the following equation:

$$\mathbf{v}^P = \mathbf{v}^O + \boldsymbol{\omega}^A \times (\mathbf{p} + \mathbf{u}) + {}^A\mathbf{v}^P, \tag{12}$$

where $\mathbf{v}^O$ is the velocity of point O which is the reference point fixed in the rigid frame A; $\boldsymbol{\omega}^A$ is the angular velocity of the rigid frame A; $\mathbf{p}$ is the position vector from O to P_0; and ${}^A\mathbf{v}^P$ is

the relative velocity of P observed from the rigid frame A, which can be obtained by taking the time derivative of $\mathbf{u}$ in the rigid frame A. By using the component notation, $\mathbf{v}^O$, $\boldsymbol{\omega}^A$, $\mathbf{p}$ and ${}^A\mathbf{v}^P$ can be expressed as follows:

$$\mathbf{v}^O = v_1\hat{a}_1 + v_2\hat{a}_2 + v_3\hat{a}_3, \tag{13}$$

$$\boldsymbol{\omega}^A = \omega_1\hat{a}_1 + \omega_2\hat{a}_2 + \omega_3\hat{a}_3, \tag{14}$$

$$\mathbf{p} = x\hat{a}_1 + y\hat{a}_2, \tag{15}$$

$${}^A\mathbf{v}^P = \dot{u}_1\hat{a}_1 + \dot{u}_2\hat{a}_2 + \dot{u}_3\hat{a}_3. \tag{16}$$

By substituting equations (13)–(16) into equation (12), the velocity of point P can be obtained as follows:

$$\begin{aligned}\mathbf{v}^P = {} & [v_1 + \dot{u}_1 + \omega_2 u_3 - \omega_3(y + u_2)]\hat{a}_1 \\ & + [v_2 + \dot{u}_2 + \omega_3(x + u_1) - \omega_1 u_3]\hat{a}_2 \\ & + [v_3 + \dot{u}_3 + \omega_1(y + u_2) - \omega_2(x + u_1)]\hat{a}_3.\end{aligned} \tag{17}$$

Since u_1 and u_2 shown in equation (17) are not approximated, they need to be replaced by s, r, and u_3. The geometric relations between the in-plane stretch variables and the Cartesian deformation variables are given as follows:

$$x + s = \int_0^x \left[\left(1 + \frac{\partial u_1}{\partial \xi}\right)^2 + \left(\frac{\partial u_3}{\partial \xi}\right)^2\right]^{1/2} \mathrm{d}\xi, \tag{18}$$

$$y + r = \int_0^y \left[\left(1 + \frac{\partial u_2}{\partial \eta}\right)^2 + \left(\frac{\partial u_3}{\partial \eta}\right)^2\right]^{1/2} \mathrm{d}\eta. \tag{19}$$

By using the binomial expansion theorem (since linear equations of motion are to be derived eventually), the above two equations can be approximated (without affecting the final results) as follows:

$$s = u_1 + \tfrac{1}{2}\int_0^x \left[\left(\frac{\partial u_3}{\partial \xi}\right)^2\right] \mathrm{d}\xi, \tag{20}$$

$$r = u_2 + \tfrac{1}{2}\int_0^y \left[\left(\frac{\partial u_3}{\partial \eta}\right)^2\right] \mathrm{d}\eta. \tag{21}$$

Differentiations of equations (20) and (21) with respect to time yield

$$\dot{s} = \dot{u}_1 + \int_0^x \left[\left(\frac{\partial \dot{u}_3}{\partial \xi}\right)\left(\frac{\partial u_3}{\partial \xi}\right)\right] \mathrm{d}\xi, \tag{22}$$

$$\dot{r} = \dot{u}_2 + \int_0^y \left[\left(\frac{\partial \dot{u}_3}{\partial \eta}\right)\left(\frac{\partial u_3}{\partial \eta}\right)\right] \mathrm{d}\eta. \tag{23}$$

Thus, $\dot{u}_1$ and $\dot{u}_2$ in equation (17) can be replaced by $\dot{s}$, $\dot{r}$, and $\dot{u}_3$. By using equations (22) and (23) along with equations (17) and (1)–(3), the partial derivative of $\mathbf{v}^P$ with respect to $\dot{q}_i$ can be

obtained as follows:

$$\frac{\partial \mathbf{v}^P}{\partial \dot{q}_i} = \left[\phi_{1i} - \sum_{j=1}^{\mu} \int_0^x \phi_{3i,\xi}\phi_{3j,\xi}\,\mathrm{d}\xi\, q_i\right]\hat{a}_1 + \left[\phi_{2i} - \sum_{j=1}^{\mu} \int_0^y \phi_{3i,\eta}\phi_{3j,\eta}\,\mathrm{d}\eta\, q_j\right]\hat{a}_2 + [\phi_{3i}]\,\hat{a}_3. \tag{24}$$

By simply differentiating the velocity shown in equation (17) with respect to time, the acceleration of point P can be obtained. Then, by substituting the acceleration and the partial velocities shown in equation (24) into equation (11), the generalized inertia forces can be obtained. The substituting procedure is trivial except applying the integral by parts theorem as follows:

$$\int_0^b\int_0^a\left[\sum_{j=1}^{\mu}\int_0^x \phi_{3i,\xi}\phi_{3j,\xi}\,\mathrm{d}\xi\, q_j\right]\mathrm{d}x\,\mathrm{d}y = \sum_{j=1}^{\mu}\left[\int_0^b\int_0^a (a-x)\phi_{3i,x}\phi_{3j,x}\,\mathrm{d}x\,\mathrm{d}y\right]q_j, \tag{25}$$

$$\int_0^b\int_0^a\left[\sum_{j=1}^{\mu}\int_0^y \phi_{3i,\eta}\phi_{3j,\eta}\,\mathrm{d}\eta\, q_j\right]\mathrm{d}x\,\mathrm{d}y = \sum_{j=1}^{\mu}\left[\int_0^b\int_0^a (b-y)\phi_{3i,y}\phi_{3j,y}\,\mathrm{d}x\,\mathrm{d}y\right]q_j, \tag{26}$$

$$\int_0^b\int_0^a x\left[\sum_{j=1}^{\mu}\int_0^x \phi_{3i,\xi}\phi_{3j,\xi}\,\mathrm{d}\xi\, q_j\right]\mathrm{d}x\,\mathrm{d}y = \sum_{j=1}^{\mu}\left[\int_0^b\int_0^a \tfrac{1}{2}(a^2-x^2)\phi_{3i,x}\phi_{3j,x}\,\mathrm{d}x\,\mathrm{d}y\right]q_j, \tag{27}$$

$$\int_0^b\int_0^a y\left[\sum_{j=1}^{\mu}\int_0^y \phi_{3i,\eta}\phi_{3j,\eta}\,\mathrm{d}\eta\, q_j\right]\mathrm{d}x\,\mathrm{d}y = \sum_{j=1}^{\mu}\left[\int_0^b\int_0^a \tfrac{1}{2}(b^2-y^2)\phi_{3i,y}\phi_{3j,y}\,\mathrm{d}x\,\mathrm{d}y\right]q_j, \tag{28}$$

$$\int_0^b\int_0^a y\left[\sum_{j=1}^{\mu}\int_0^x \phi_{3i,\xi}\phi_{3j,\xi}\,\mathrm{d}\xi\, q_j\right]\mathrm{d}x\,\mathrm{d}y = \sum_{j=1}^{\mu}\left[\int_0^b\int_0^a y(a-x)\phi_{3i,x}\phi_{3j,x}\,\mathrm{d}x\,\mathrm{d}y\right]q_j, \tag{29}$$

$$\int_0^b\int_0^a x\left[\sum_{j=1}^{\mu}\int_0^y \phi_{3i,\eta}\phi_{3j,\eta}\,\mathrm{d}\eta\, q_j\right]\mathrm{d}x\,\mathrm{d}y = \sum_{j=1}^{\mu}\left[\int_0^b\int_0^a x(b-y)\phi_{3i,y}\phi_{3j,y}\,\mathrm{d}x\,\mathrm{d}y\right]q_j. \tag{30}$$

Finally, the generalized inertia forces are linearized to obtain the following linear equations of motion:

$$\sum_{j=1}^{\mu}\left[M_{ij}^{11}\ddot{q}_j + (K_{ij}^{S1}+K_{ij}^{S2})q_j + (\omega_1\omega_2-\dot{\omega}_3)M_{ij}^{12}q_j + (\omega_3\omega_1+\dot{\omega}_2)M_{ij}^{13}q_j - (\omega_2^2+\omega_3^2)M_{ij}^{11}q_j - 2\omega_3 M_{ij}^{12}\dot{q}_j + 2\omega_2 M_{ij}^{13}\dot{q}_j\right] = (\omega_2^2-\omega_3^2)X_{1i} - (\omega_1\omega_2-\dot{\omega}_3)Y_{1i} - (\dot{v}_1+\omega_2 v_3-\omega_3 v_2)Z_{1i}, \tag{31}$$

$$\sum_{j=1}^{\mu}\left[M_{ij}^{22}\ddot{q}_j + (K_{ij}^{S3}+K_{ij}^{S4})q_j + (\omega_1\omega_2-\dot{\omega}_3)M_{ij}^{21}q_j + (\omega_2\omega_3-\dot{\omega}_1)M_{ij}^{23}q_j - (\omega_3^2+\omega_1^2)M_{ij}^{22}q_j + 2\omega_3 M_{ij}^{21}\dot{q}_j - 2\omega_1 M_{ij}^{23}\dot{q}_j\right] = (\omega_1\omega_2+\dot{\omega}_3)X_{2i} + (\omega_3^2+\omega_1^2)Y_{2i} - (\dot{v}_2+\omega_3 v_1-\omega_1 v_3)Z_{2i}, \tag{32}$$

$$\sum_{j=1}^{\mu}\Big[M_{ij}^{33}\ddot{q}_j + K_{ij}^{B}q_j - (\omega_1^2+\omega_2^2)M_{ij}^{33}q_j + (\omega_3\omega_1+\dot{\omega}_2)M_{ij}^{31}q_j$$

$$+ (\omega_2\omega_3+\dot{\omega}_1)M_{ij}^{32}q_j + 2\omega_1 M_{ij}^{32}\dot{q}_j - 2\omega_2 M_{ij}^{31}\dot{q}_j$$

$$+ (\omega_2^2+\omega_3^2)K_{ij}^{GX2}q_j - (\dot{v}_1+\omega_2 v_3-\omega_3 v_2)K_{ij}^{GX1}q_j + (\omega_3^2+\omega_1^2)K_{ij}^{GY2}q_j$$

$$- (\dot{v}_2+\omega_3 v_1-\omega_1 v_3)K_{ij}^{GY1}q_j - (\omega_1\omega_2-\dot{\omega}_3)K_{ij}^{GXY}q_j\Big]$$

$$= -(\omega_3\omega_1-\dot{\omega}_2)X_{3i} - (\omega_2\omega_3+\dot{\omega}_1)Y_{3i} - (\dot{v}_3+\omega_1 v_2-\omega_2 v_1)Z_{3i}, \tag{33}$$

where

$$M_{ij}^{lm} = \int_0^b\int_0^a \rho\phi_{li}\phi_{mj}\,\mathrm{d}x\,\mathrm{d}y, \tag{34}$$

$$K_{ij}^{S1} = \int_0^b\int_0^a (\beta_1\phi_{1i,x}\phi_{1j,x} + \beta_2\phi_{1i,y}\phi_{1j,y})\,\mathrm{d}x\,\mathrm{d}y, \tag{35}$$

$$K_{ij}^{S2} = \int_0^b\int_0^a (\beta_1 v\phi_{1i,x}\phi_{2j,y} + \beta_2\phi_{1i,y}\phi_{2j,y})\,\mathrm{d}x\,\mathrm{d}y, \tag{36}$$

$$K_{ij}^{S3} = \int_0^b\int_0^a (\beta_1\phi_{2i,y}\phi_{2j,y} + \beta_2\phi_{2i,x}\phi_{2j,x})\,\mathrm{d}x\,\mathrm{d}y, \tag{37}$$

$$K_{ij}^{S4} = \int_0^b\int_0^a (\beta_1 v\phi_{2i,x}\phi_{1j,y} + \beta_2\phi_{2i,y}\phi_{1j,x})\,\mathrm{d}x\,\mathrm{d}y, \tag{38}$$

$$K_{ij}^{B} = \int_0^b\int_0^a \beta_3\Big[\phi_{3i,xx}\phi_{3j,xx} + \phi_{3i,yy}\phi_{3j,yy} + v\phi_{3i,xx}\phi_{3j,yy}$$

$$+ v\phi_{3i,yy}\phi_{3j,xx} + 2(1-v)\phi_{3i,xy}\phi_{3j,xy}\Big]\mathrm{d}x\,\mathrm{d}y, \tag{39}$$

$$K_{ij}^{GX2} = \int_0^b\int_0^a \tfrac{1}{2}\rho(a^2-x^2)\phi_{3i,x}\phi_{3j,x}\,\mathrm{d}x\,\mathrm{d}y, \tag{40}$$

$$K_{ij}^{GX1} = \int_0^b\int_0^a \rho(a-x)\phi_{3i,x}\phi_{3j,x}\,\mathrm{d}x\,\mathrm{d}y, \tag{41}$$

$$K_{ij}^{GY2} = \int_0^b\int_0^a \tfrac{1}{2}\rho(b^2-y^2)\phi_{3i,y}\phi_{3j,y}\,\mathrm{d}x\,\mathrm{d}y, \tag{42}$$

$$K_{ij}^{GY1} = \int_0^b\int_0^a \rho(b-y)\phi_{3i,y}\phi_{3j,y}\,\mathrm{d}x\,\mathrm{d}y, \tag{43}$$

$$K_{ij}^{GXY} = \int_0^b \int_0^a \rho \left[x(b-y)\phi_{3i,y}\phi_{3j,y} + y(a-x)\phi_{3i,x}\phi_{3j,x} \right] \mathrm{d}x\,\mathrm{d}y, \tag{44}$$

$$X_{mi} = \int_0^b \int_0^a \rho x \phi_{mi}\,\mathrm{d}x\,\mathrm{d}y, \tag{45}$$

$$Y_{mi} = \int_0^b \int_0^a \rho y \phi_{mi}\,\mathrm{d}x\,\mathrm{d}y, \tag{46}$$

$$Z_{mi} = \int_0^b \int_0^a \rho \phi_{mi}\,\mathrm{d}x\,\mathrm{d}y. \tag{47}$$

The stiffness matrix elements shown in equations (40)–(44) are used for the five motion-induced stiffness variation terms in equation (33), which do not appear if the conventional linear modelling method is employed to derive the equations of motion. Due to the lack of these terms, the conventional linear modelling method often produces erroneous results for the dynamic analysis of plates undergoing overall motion. As shown in equation (33), the five motion-induced stiffness variation terms are expressed as functions of the overall motion of the plate, which consists of translational, Coriolis, and centrifugal acceleration components. It can also be found that those acceleration components cause in-plane stretching of the plate. Therefore, one can conclude that the conventional linear modelling method can be used reliably unless the overall motion of the plate causes in-plane stretching.

Equations (31)–(33) can be used for the transient analysis of a plate undergoing overall motion. If the coupling effect between stretching and bending motions is negligible, equation (33) can be used independently after ignoring all the coupling terms appearing in the equation. Since the natural frequencies of stretching modes are usually much higher than those of bending modes, equation (33) can be also used for the bending vibration analysis of a plate undergoing overall motion.

3. NUMERICAL RESULTS

Figure 3 shows a rectangular cantilever plate. The geometric and the material data for the plate are given in Table 1. The plate is attached to a rigid hub which undergoes a rotational motion. The angular speed of the plate is given as follows:

$$\begin{gathered} \Omega = \Omega_s \left(\frac{t}{T_s} - \frac{1}{2\pi} \sin \frac{2\pi t}{T_s} \right) \quad (0 \leqslant t \leqslant T_s), \\ \Omega = \Omega_s \quad (t > T_s). \end{gathered} \tag{48}$$

This function is often called a spin-up function which increases very smoothly and reaches a steady state angular speed. After reaching the steady state angular speed, the angular speed is maintained constant. Since this function has the varying region as well as the constant region, it is often employed to represent a general prescribed motion. Ω_s and T_s in equation (48) represent the steady state angular speed and the time required to reach the steady state angular speed respectively.

Figure 4 and 5 show the lateral deflection (measured with respect to the rotating rigid frame) of the point P which is located at the free end of the cantilever plate. Five seconds is used for T_s and 10 and 20 rad/s are used for Ω_s to obtain the results shown in Figures 4 and

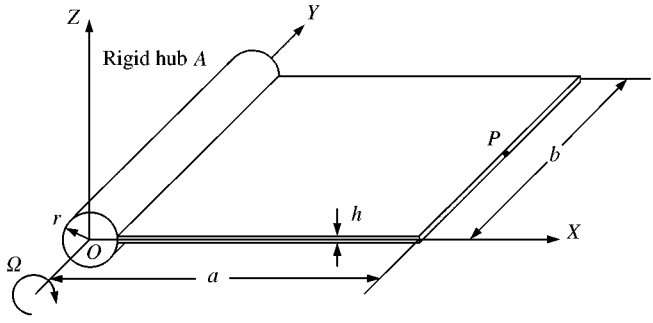

Figure 3. Rectangular plate undergoing rotational motion.

TABLE 1

The geometric and the material data for the plate

Notation	Data
Length a	1·0 m
Width b	0·5 m
Thickness h	0·0025 m
Radius r	0·0 m
Young's modulus E	7·0E10 N/m^2
Shear modulus G	2·7E10 N/m^2
Poisson's ratio v	0·3
Mass per unit area ρ	7·5 kg/m^2

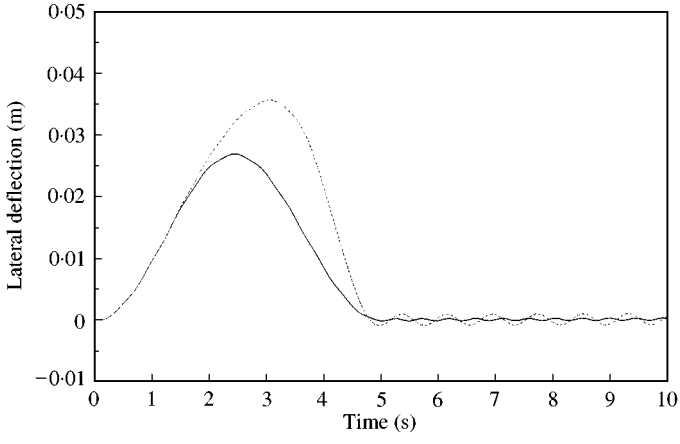

Figure 4. Numerical results obtained by present and conventional modelling methods (for the case of $\Omega_s = 10$ rad/s). ——, Present modelling; ·····, Conventional modelling.

5 respectively. The results in Figures 4 and 5 are obtained by the present authors. It is shown that the results obtained by the present modelling method are significantly different from those obtained by the conventional linear modelling method. Figure 5 shows that the conventional linear modelling method even provides an improper divergent response. This improper estimation results from the lack of the five motion-induced stiffness variation

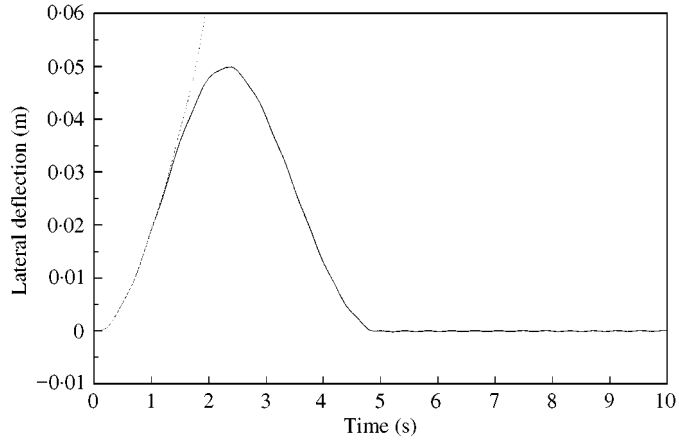

Figure 5. Numerical results obtained by present and conventional modelling methods (for the case of $\Omega_s = 20$ rad/s). ——, Present modelling; ·····, Conventional modelling.

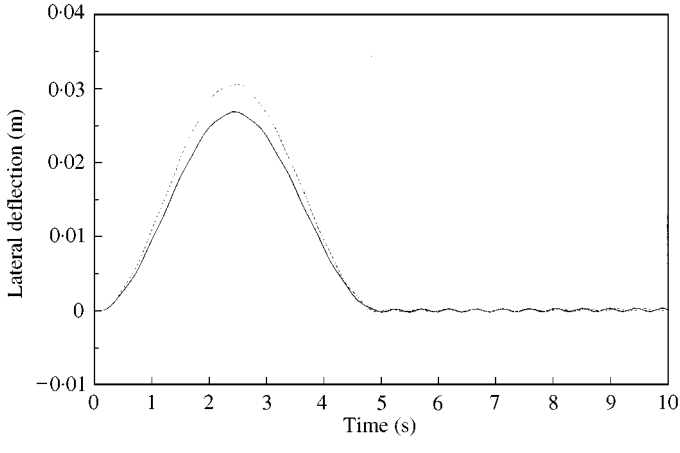

Figure 6. Numerical results obtained by the plate and the beam modelling methods (for the case of $\Omega_s = 10$ rad/s). ——, Plate modelling; ·····, Beam modelling.

terms shown in equation (33). While the motion-induced stiffness variation terms are absent from the equations of motion obtained by using the conventional linear modelling method, the third term in equation (33) (which softens the system as the angular speed increases) remains in the equations of motion and causes the divergent response.

In Figures 6 and 7, the results obtained by using the present modelling method are compared with those obtained by using a beam-modelling method, which proved to be accurate in references [9, 10]. It is shown that the lateral deflections obtained by using the present modelling method (for plates) are a little bit smaller than those obtained by using the beam-modelling method. The difference results from the Poisson's ratio effect which is only active for plate theories. These results exhibit the reliability of the present modelling method for plates undergoing overall motion.

Now, the natural frequencies of the rectangular cantilever plate (shown in Figure 3) are obtained and shown in Table 2. The plate is assumed to be rotating with the steady state angular speeds. Therefore, in the equation (33), $\omega_2 = \Omega_s$ and $v_3 = -r\Omega_s$. All the other

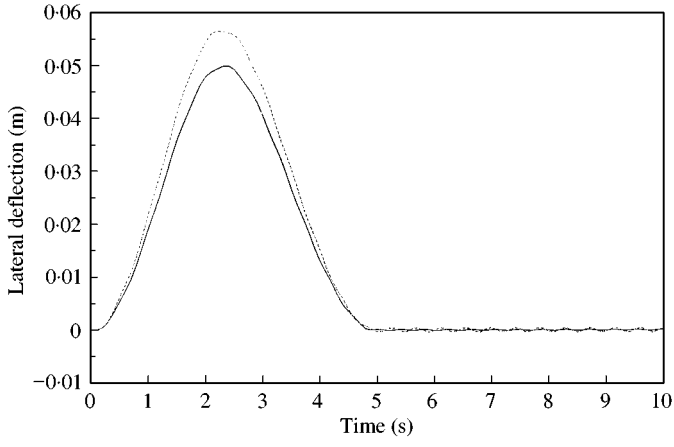

Figure 7. Numerical results obtained by the plate and the beam modelling methods (for the case of $\Omega_s = 20$ rad/s). ——, Plate modelling; ·····, Beam modelling.

TABLE 2

The natural frequencies of the rectangular Cantilever plate

Angular speed Ω_s (rad/s)	Mode	Southwell (Hz)	Present (Hz)
10	1	2·1243	2·1297
	2	8·6299	8·6439
	3	13·084	13·081
	4	28·406	28·416
	5	35·761	35·778
20	1	2·4167	2·4031
	2	8·6326	8·6871
	3	14·593	14·583
	4	29·180	29·213
	5	37·430	37·488

overall motion components are set to zero. The lowest five natural frequencies of the plate obtained by using the present modelling method are compared with those obtained by the Southwell's method (see reference [12]). The table shows reasonable agreement between the two results.

Now to show the three-dimensional analysis capability of the present modelling method, a more sophisticated example is given in Figure 8. The cantilever plate shown in the figure is attached to a rigid hub, which is rotating with a spin-up angular velocity. The distance (denoted as r in Figure 8) from the rotation axis to the reference point O is 0·2 m. Two co-ordinate systems are attached to the rigid hub. $\hat{a}_1$ and $\hat{a}_2$ are parallel to the length and the width of the undeformed rectangular plate and $\hat{a}_3$ is perpendicular to the plate. $\hat{b}_i$'s constitute another co-ordinate system in which $\hat{b}_2$ is parallel to the axis of rotation. The co-ordinate system $\hat{a}_i$'s can be obtained by 1–2–3 space rotation of $\hat{b}_i$'s. The three rotation angles are often called Euler angles and their respective values are 15, 0 and 30° in this example. The other geometrical and the material data are same as those given in Table 2. Figures 9 and 10 show the lateral deflections of point P which locates at a corner of the free end of the cantilever plate. Ω_s is 10 rad/s and T_s is 5 or 1 s. Results obtained by using the present modelling method and the conventional linear modelling method are compared in

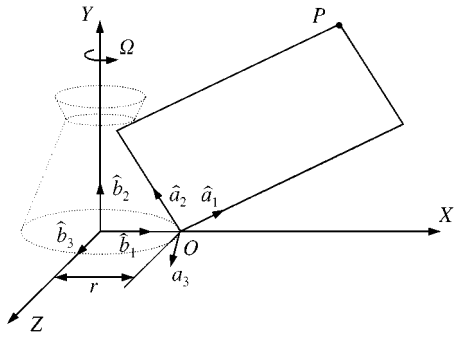

Figure 8. More sophisticated example of plate undergoing overall motion.

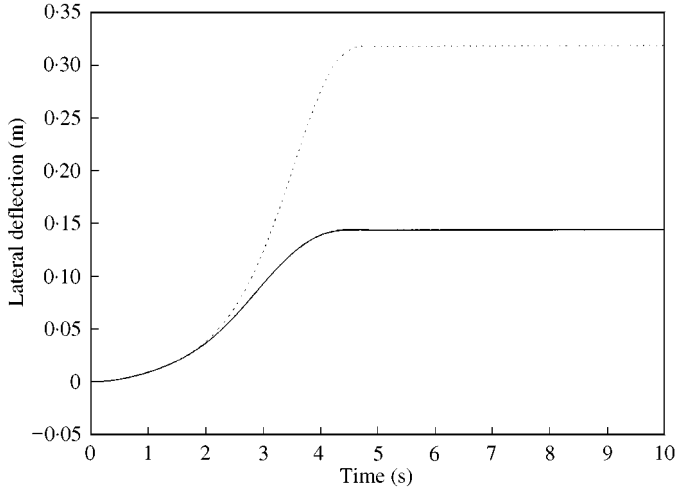

Figure 9. Numerical results obtained by present and conventional modelling methods (for the case of $\Omega_s = 10$ rad/s and $T_s = 5$ s). ——, Present modelling; ·····, Conventional modelling.

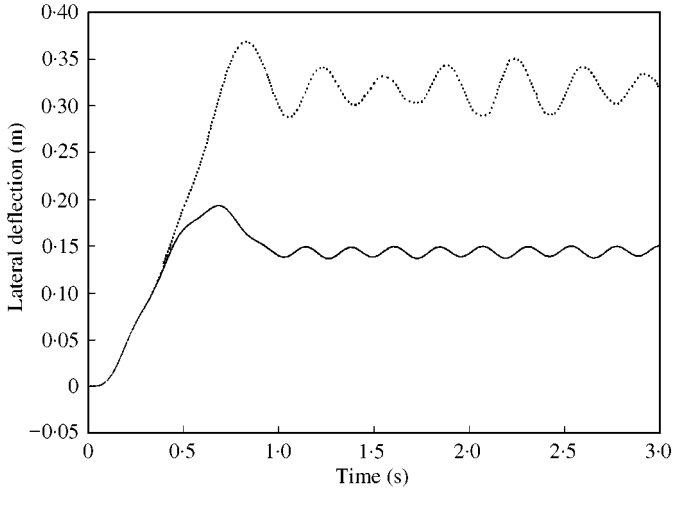

Figure 10. Numerical results obtained by present and conventional modelling methods (for the case of $\Omega_s = 10$ rad/s and $T_s = 1$ s). ——, Present modelling; ·····, Conventional modelling.

the figure. These results indicate that significant error may occur if the conventional linear modelling method is employed to obtain the dynamic response of a plate undergoing overall motion. Figure 10 also shows that the maximum deflection overshoots the steady state mean deflection and oscillation occurs at the steady state if an abrupt spin-up motion (meaning small time constant T_s) is prescribed. Some sample numerical data, which are presented in Figures 9 and 10, are provided in Table 3 for later comparison study.

Figure 11 shows five pictures (at five successive instants) of the above example obtained by the present modelling method. Overall response of the plate can be observed easily with

TABLE 3

Sample numerical data by the present modelling method

Time (t/T_s)	Lateral deflection of point P	
	$T_s = 5$	$T_s = 1$
0·0	0·00000	0·00000
0·2	0·00008	0·04549
0·4	0·00031	0·12870
0·6	0·00068	0·18332
0·8	0·00119	0·17055
1·0	0·00181	0·13972
1·2	0·00257	0·14351
1·4	0·00346	0·14811
1·6	0·00452	0·14939
1·8	0·00579	0·14499
2·0	0·00731	0·14159

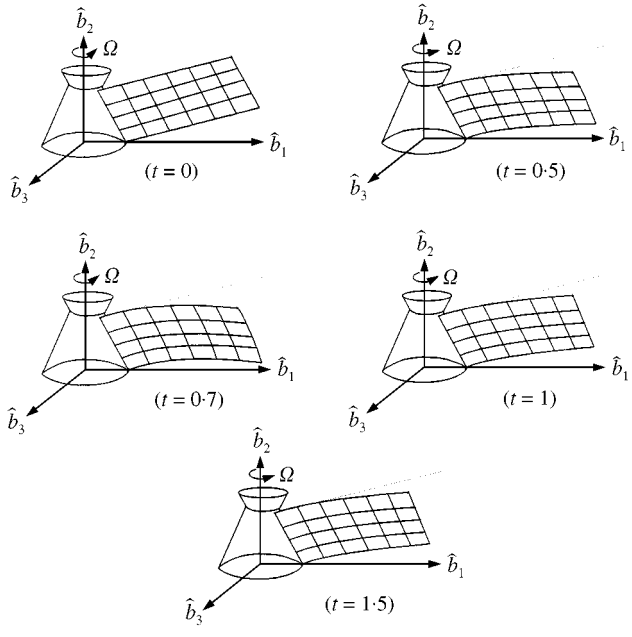

Figure 11. Dynamic deformation of the rotating plate with respect to time (for the case of $\Omega_s = 10$ rad/s and $T_s = 1$ s).

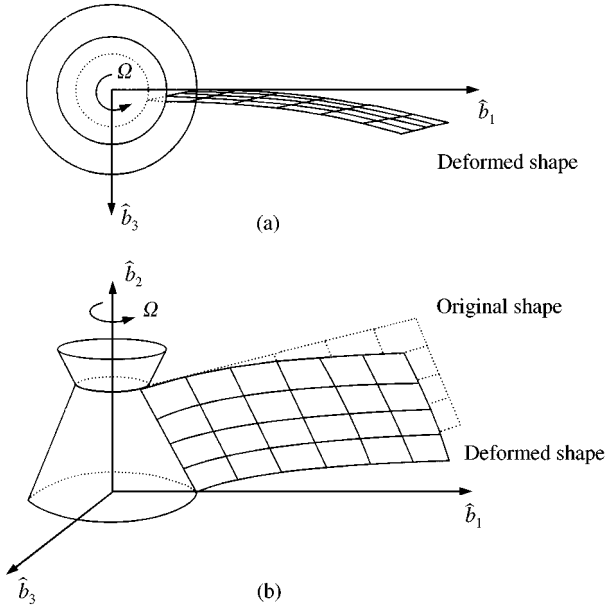

Figure 12. Steady state deformed shape of the rotating plate. (a) Top view; (b) Perspective view.

these pictures. Figure 12 shows the steady state deformed shape of the plate. The numbers of mode functions for s, r, and u_3 (to obtain the transient results of plate presented so far) are 2, 2 and 5 respectively. Those numbers were confirmed to be sufficient to achieve the convergence for the transient results.

4. CONCLUSIONS

A linear modelling method for the dynamic analysis of a rectangular plate undergoing prescribed overall motion is presented in this paper. The modelling method employs two stretch variables by which the in-plane strain energy of a plate can be expressed in an exact quadratic form. Different from the conventional linear modelling method, proper motion-induced stiffness variation terms are included in the equations of motion obtained by the present modelling method. Numerical study shows that the motion-induced stiffness variation terms may significantly affect the dynamic response of a plate undergoing overall motion. The reliability and the accuracy of the present modelling method is verified through transient and vibration analysis of a rectangular plate undergoing rotational motion.

ACKNOWLEDGMENTS

This research was supported by Center of Innovative Design Optimization Technology (ERC of Korea Science and Engineering Foundation).

REFERENCES

1. C. Bodley, A. Devers, A. Park and H. Frisch 1978 *NASA TP* 1219. A Digital computer program for the dynamic interaction simulation of controls and structure (DISCOS).

2. H. FRISCH 1975 *NASA TN* D-8047. A vector-dyadic development of the equations of motion for N-coupled flexible bodies and point masses.
3. J. HO 1997 *Journal of Spacecraft and Rockets* **14**, 102–110. Direct path method for flexible multibody spacecraft dynamics.
4. W. HURTY, J. COLLINS and G. HART 1971 *Computers and Structures* **1**, 553–563. Dynamic analysis of large structures by modal synthesis techniques.
5. E. CHRISTENSEN and S. LEE 1986 *Computers and Structures* **23**, 819–829. Nonlinear finite element modeling of the dynamics of unrestrained flexible structures.
6. T. BELYTSCHKO and B. HSIEH 1973 *International Journal of Numerical Methods Engineering* **7**, 255–271. Nonlinear transient finite element analysis with convected coordinates.
7. J. SIMO and L. VU-QUOC 1986 *Journal of Applied Mechanics* **53**, 849–863. On the dynamics of flexible beams under large overall motions—the plane case: parts I and II.
8. S. WU and E. HAUG 1998 *International Journal of Numerical Methods Engineering* **26**, 2211–2226. Geometric nonlinear substructuring for dynamics of flexible mechanical systems.
9. T. KANE, R. RYAN and A. BANERJEE 1987 *Journal of Guidance, Control, and Dynamics* **10**, 139–151. Dynamics of a Cantilever beam attached to a moving base.
10. H. YOO, R. RYAN and R. SCOTT 1994 *Journal of Sound and Vibration* **10**, 139–148. Dynamics of flexible beams undergoing overall motions.
11. J. SIMO and L. VU-QUOC 1987 *Journal of Sound and Vibration* **119**, 487–508. The role of non-linear theories in transient dynamic analysis of flexible structures.
12. M. DOKAINISH and S. RAWTANI 1971 *International Journal of Numerical Methods Engineering* **3**, 233–248. Vibration analysis of rotating Cantilever plates.
13. V. RAMAMURTI and R. KIELB 1984 *Journal of Sound and Vibration* **97**, 429–449. Natural frequencies of twisted rotating plates.
14. A. LEISSA 1969 *NASA SP* 160. Vibration of plates.
15. T. KANE and D. LEVINSON 1985 New York: McGraw-Hill. *Dynamics: Theory and Applications.*